

Free Convective Heat Transfer in a Partially Open Cavity

Francesco Devia, Mario Misale, Giovanni Tanda.

Dipartimento di Termoeconomica e Condizionamento Ambientale (DITEC)

Università degli Studi di Genova,

via all'Opera Pia 15/a - I-16145 GENOVA (ITALY)

Summary

Natural air ventilation in partially open cavities is encountered in many practical applications such as energy conservation in buildings and the heating/cooling of environmental systems. In this work, natural convection heat transfer in a partially open cavity is analysed. A vertical isothermal plate, placed inside the cavity, acts as the thermal source promoting the buoyant air flow drawn into the cavity through vent openings. Experiments encompassed the determination of the local and average convective heat transfer coefficients for the heated plate by means of the schlieren optical technique.

Introduction

The need for information on the thermal behaviour of natural convective flow in channels and cavities has been recognised by the building design community. This applies, for instance, to passive solar heating, Trombe walls, and natural ventilation systems as documented by several studies reported in the literature (1-7). The main advantage of natural convection is its intrinsic reliability, because the air movement is simply generated by local density gradients in the presence of the gravitational field. The thermal design of a naturally ventilated device depends on geometric and operating conditions: shape and dimensions of the system, flow areas of the inlet/outlet openings, location of the heat sources, amount of thermal power dissipated, chimney height, and so on (8). Owing to the large number of parameters involved, experiments are of great importance in understanding the thermal behaviour of naturally ventilated systems. Despite this consideration, a literature survey revealed only few experimental works devoted to natural convection in partially open cavities.

The present paper reports the study of the heat transfer characteristics of a naturally ventilated, rectangular cavity in which a vertical, isothermal plate is placed. The plate, heated by the Joule effect,

is symmetrical with the lateral walls of the cavity to form two adjacent, identical, vented channels. The cavity has lateral, rectangular openings to enable the plate to be cooled by the natural convection of ambient air.

The air movement induced by the test section arrangement is similar to that encountered in several heating and ventilation systems. For example, the heated plate can simulate the massive wall of a simplified Trombe wall system that can be used for the passive heating (1,2) or cooling of houses (5,7). Moreover the channel between the heated plate and the cavity wall can be representative of a glazing/frame assembly (a blind or shading device adjacent to the indoor surface of a window) where the reduction of the thermal conductance is the major concern (6).

The experiments were conducted by parametrically varying the spacing between the plate and the cavity walls (i.e. the channel width), the location and size of the openings, the thermal conductance of the unheated cavity walls and the plate-to-ambient temperature difference. For some cavity configurations, numerical simulations by using a commercial finite-element code were performed and results checked against experimental data.

Owing to the diverse possible applications of the study, one of the objectives of this work is to recast the obtained data in dimensionless form and present them by using dimensionless groups in order to extend their validity to the full-scale geometry of the passive heating/cooling device.

The experiments

A schematic view of the test section is presented in Fig.1. A vertical, isothermal plate is bounded by two lateral, vertical, unheated walls to form a cavity. The height H of the plate is 10 cm; the other dimensions are: thickness $D=1$ cm, length $L=50$ cm. The inner dimensions of the cavity are: height $H_c=16$ cm, length $L_c=53$ cm. The inner width W_c of the cavity was varied from 2.0 to 5.2 cm in order to have three values of the interwall spacing to plate height ratio W/H ; namely $W/H=0.05$, 0.1 and 0.21. The lateral walls have openings to permit cooling of the plate by natural ventilation.. The experiments were conducted by considering two rectangular openings for each side with the height H' varying from 0.5 to 2 cm, the length being kept equal to 52 cm. The ambient air enters the cavity from the bottom opening and the heated air is discharged from the top opening. Supplementary experiments were performed by considering the presence of an additional rectangular opening on each lateral wall, the height of all the openings being kept equal to 1 cm.

The plate was made of two aluminium sheets with a plane heater sandwiched in between. Aluminium was chosen because of its high thermal conductivity which ensures a good degree of temperature uniformity. Fourteen fine-gauge, pre-calibrated (to ± 0.1 K) thermocouples were fitted in holes drilled into the material in order to evaluate the average wall temperature as the arithmetic mean of the

Table 1. Dimensions and location of the cavity openings.

config	No. openings on each side	H' mm	H'' mm	x_{in} mm	x_{out} mm	x_{mid} mm
a	2	5	-	-5	-5	-
b	2	10	-	0	0	-
c	2	15	-	+5	+5	-
d	2	20	-	+10	+10	-
e1	3	10	10	0	0	25
e2	3	10	10	0	0	35
e3	3	10	10	0	0	45
e4	3	10	10	0	0	65

presented in (9,10). Owing to the symmetry of the configuration, the distributions of the heat transfer coefficient h were expected to be the same on both sides of the heated plate, at a given vertical location. In order to minimise the experimental errors, for each run the distribution of h was assumed as the average between the left and the right distributions. The uncertainty (at the 95% confidence level) in the h values thus estimated was found to be in the 6-14% range. The average heat transfer coefficient h_{av} was evaluated by numerically integrating the measured local values on the vertical sides; this value was always compared with that deduced by applying an energy balance (power input = overall convective heat transfer rate + thermal radiation to the surroundings) to the heated plate. Differences between the average heat transfer coefficients evaluated according to these two procedures were generally found within 10%.

Results and discussion

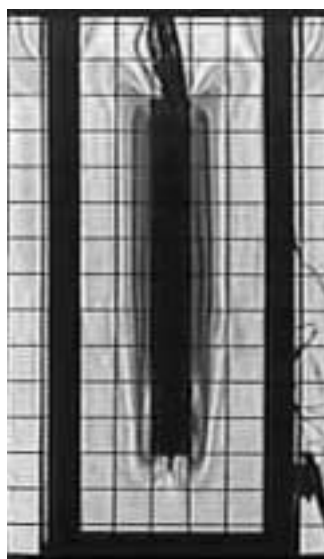


Figure 2. Typical schlieren image of the heated plate inside the partially open cavity.

The experimental heat transfer results are presented in dimensionless form. Local and average heat transfer coefficients were normalised in order to give the local and average Nusselt numbers, respectively defined as:

$$Nu = h H / k$$

$$Nu_{av} = h_{av} H / k$$

The Rayleigh number was also introduced:

$$Ra = (\beta g / \nu \alpha) H^3 (T_w - T_\infty)$$

Furthermore, some data were recast in terms of "channel" Nusselt and Rayleigh numbers defined as:

$$Nu_{ch} = Nu_{av} (W/H) = h_{av} W / k$$

$$Ra_{ch} = (W/H)^4 Ra = (W/H) (\beta g / \nu \alpha) W^3 (T_w - T_\infty)$$

The thermophysical properties of air were evaluated at the film temperature $(T_w + T_\infty)/2$.

Figure 3 shows the isotherms, in terms of the dimensionless temperature $\theta = (T - T_\infty) / (T_w - T_\infty)$, for the largest cavity ($W/H=0.21$) and the smallest cavity ($W/H=0.05$). Two openings for each side (height $H'=15$ mm, config. **c**) are considered; the plate-to-ambient temperature difference is always 25 K. When W/H is large (Fig.3a), a considerable part of the fluid driven into the cavity remains practically unheated. For the lowest interwall spacing ($W/H=0.05$) the buoyant air flow is strongly heated: at mid-height, the cavity wall attains $\theta=0.4$ when made of Plexiglas (*N-I* case, Fig.3b) and $\theta=0.7$ when made of Plexiglas with thermal insulation (*I* case, Fig.3c). Conduction through the Plexiglas is responsible for the growth of the thermal boundary layer along the external side in the *N-I* case. The same considerations apply to results plotted in Fig.4, where the values of the local Nusselt number for the same configurations are presented. Although the general trends of the local heat transfer distributions are the same, the largest reductions in the heat transfer coefficient correspond to the lowest W/H value when the cavity walls are thermally insulated. The absence of thermal insulation alleviates the heating of the upmoving air flow because of the conduction across the Plexiglas wall and better heat transfer conditions are recovered along the upper part of the heated plate.

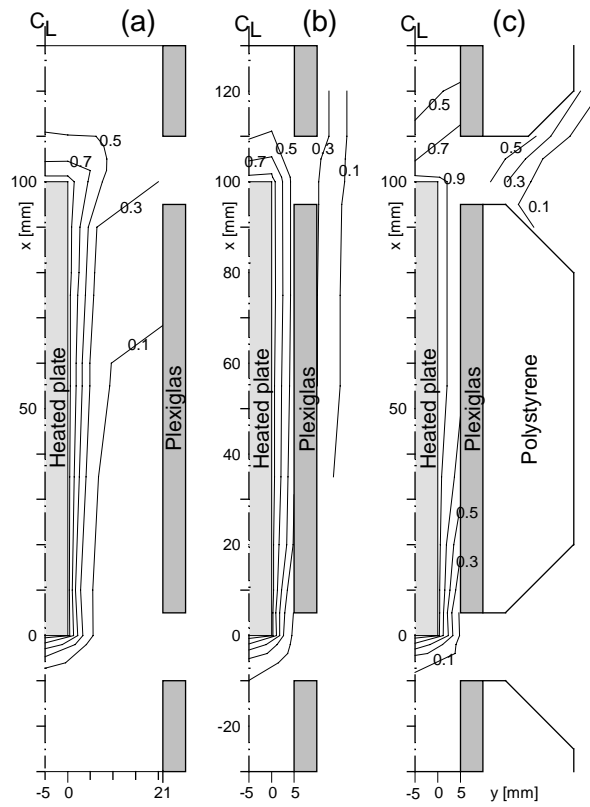


Figure 3. Isotherms (config. c) for: (a) $W/H=0.21$ (N-I case), (b) $W/H=0.05$ (N-I case) and (c) $W/H=0.05$ (I case).

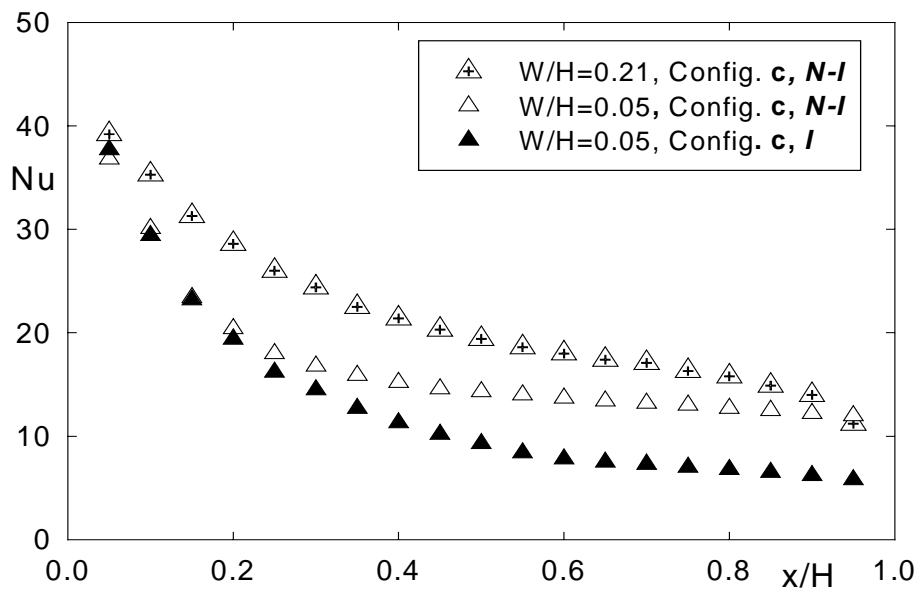


Figure 4. Local Nusselt numbers for cavity configuration c and for $W/H=0.21$, N-I case, $W/H=0.05$, N-I case and $W/H=0.05$, I case. $Ra = 2.2 \times 10^6$.

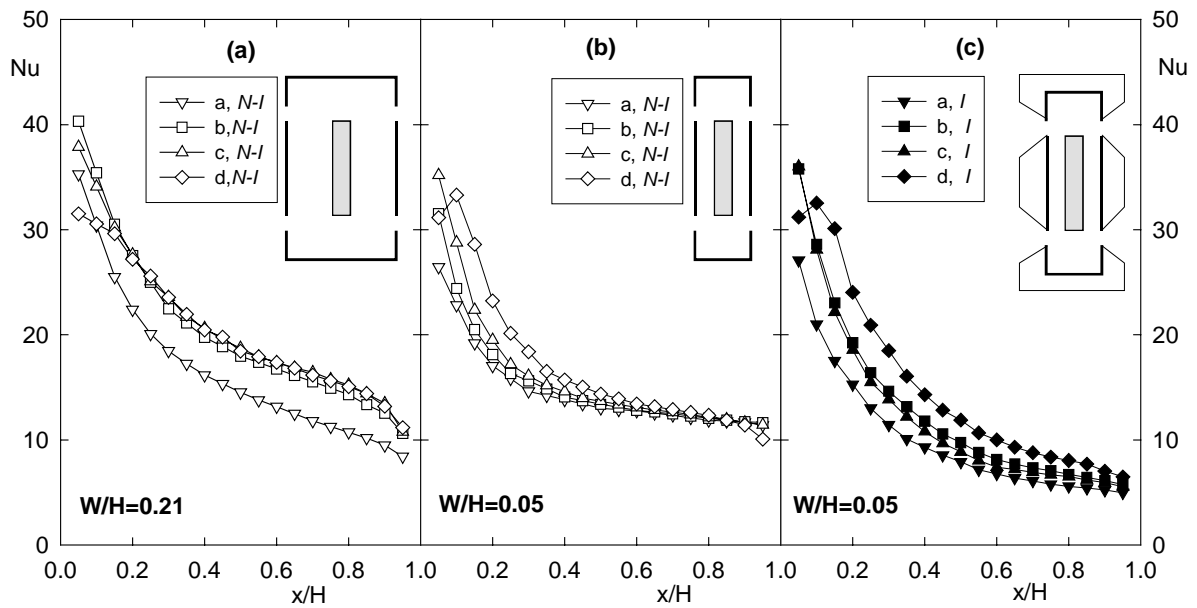


Figure 5. Effect of the height of the openings on local Nu distributions: (a) $W/H=0.21$, $N-I$ case, (b) $W/H=0.05$, $N-I$ case, (c) $W/H=0.05$, I case.

The effect of the height of the two rectangular openings on local heat transfer is shown in Fig.5a ($W/H=0.21$), Fig.5b ($W/H=0.05$, $N-I$ case), and Fig.5c ($W/H=0.05$, I case). As expected, the heat transfer coefficient is generally higher close to the leading edge of the plate and then decreases as the axial coordinate is increased. For the largest cavity ($W/H=0.21$, $N-I$), local heat transfer results plotted in Fig.5a are very close to each other, except for the smallest opening height (config. **a**), for which the local distribution shifts toward 15-20% lower values. When the interwall distance is reduced, local Nu profiles exhibit larger differences in the lower region of the plate when the cavity walls are not thermally insulated (Fig.5b) and over the whole plate when they are thermally insulated (Fig.5c). In the latter case, Nu numbers reach very low values close to trailing edge of the plate, owing to the noticeable heating of buoyant air.

The results obtained in the presence of a third opening are reported in Figs. 6-7. The graph of Fig.6 displays the Nu distributions for the cavity having $W/H=0.21$ (a) and $W/H=0.10$ (b). Data refer to a cavity with two lateral openings (height 10 mm, config. **b**) and with three lateral openings (height 10 mm) on each side. In the latter case, two axial positions of the additional opening are considered: lower (config. **e2**) and higher (config. **e4**); thus the direct comparison of the Nu profiles permits the effect of the third additional opening to be identified. Results obtained for Plexiglas walls ($N-I$ case) only are plotted since the effect of the thermal insulation of the cavity walls was found to be negligible for these W/H values. Despite the different arrangement of the openings, the Nu distributions along the plate for $W/H=0.21$ show a common behaviour, with slight differences in percentage (within $\pm 15\%$).

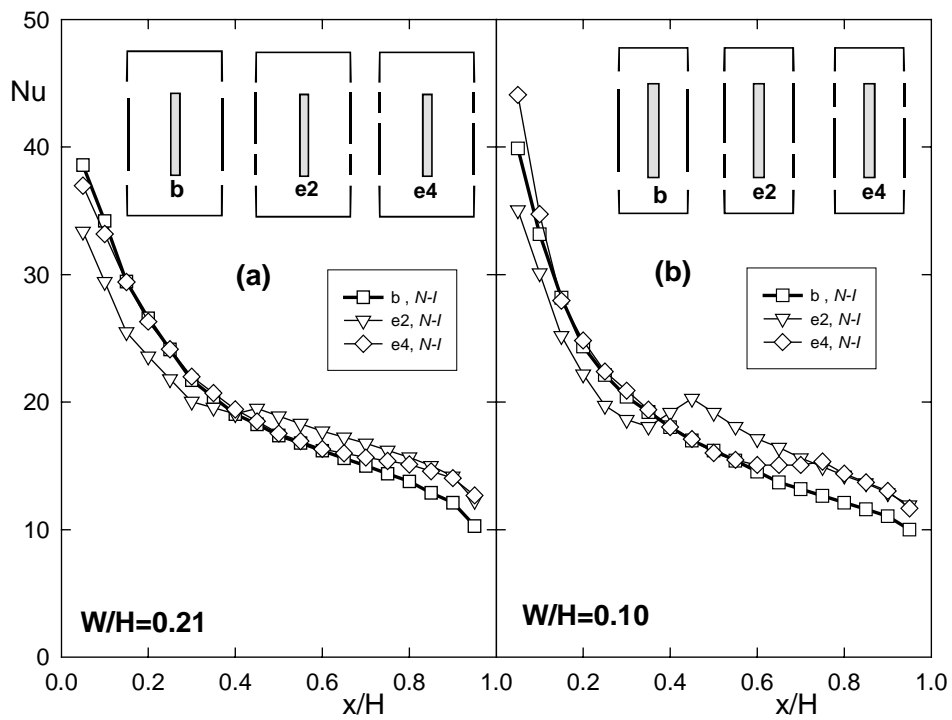


Figure 6. Effect of the third additional opening on local Nu distributions for (a) $W/H=0.21$ and (b) $W/H=0.10$. Cavity walls without thermal insulation (N-I case), $Ra = 2.2 \times 10^6$.

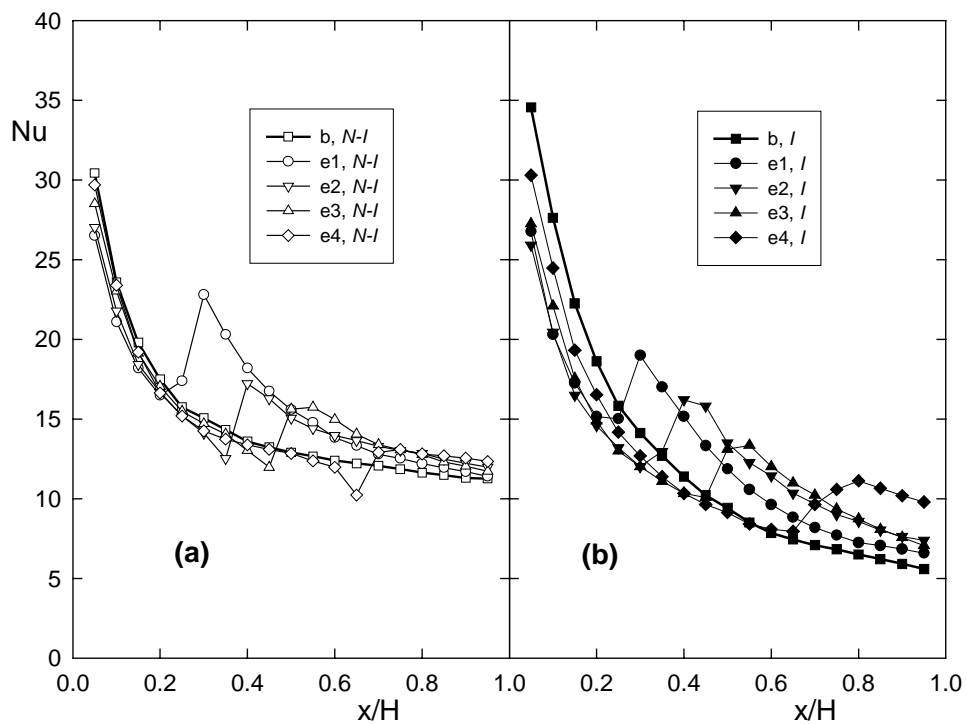


Figure 7. Effect of the third additional opening on local Nu distributions for $W/H=0.05$. Cavity walls without (a) and with (b) thermal insulation; $Ra = 2.2 \times 10^6$.

When the interwall spacing is reduced ($W/H=0.10$) the effect of the third additional opening on each side of the cavity becomes more evident, with a peak in heat transfer approximately at the same elevation as the third opening location. Figure 7 shows the Nu distributions for the smallest W/H ratio ($W/H=0.05$) and cavity walls without ($N-I$ case, Fig.7a) and with (I case, Fig. 7b) thermal insulation. Four different axial positions of the third opening are considered here, with the midheight vent coordinate increasing when passing from config.e1 to config.e4 (see Table 1).

As emerges from the inspection of Fig.7, the lateral insulation of the cavity walls plays an important role here, yielding significant reductions in Nu values as the trailing edge of the plate is approached. For each cavity configuration, a peak in the local Nusselt number is exhibited in response to the presence of the third vent opening; the relative maximum in Nu is less pronounced at vent locations higher in the cavity. It is argued that varying the location of the third opening causes the amount of cold fluid entering the bottom opening to vary, without significantly affecting the total mass flow drawn into the cavity. In order to corroborate this expectation, a few numerical simulations using the finite-element code ANSYS 5.5 have been performed. The results of the numerical simulations for cavity configurations **b**, **e2**, and **e4**, with $W/H=0.05$ and thermally insulated cavity walls (I case) were first checked against the experimental heat transfer data, as shown in Fig.8. The inspection of the figure shows similar trends for the computed and measured Nu distributions; the extent of the peak in

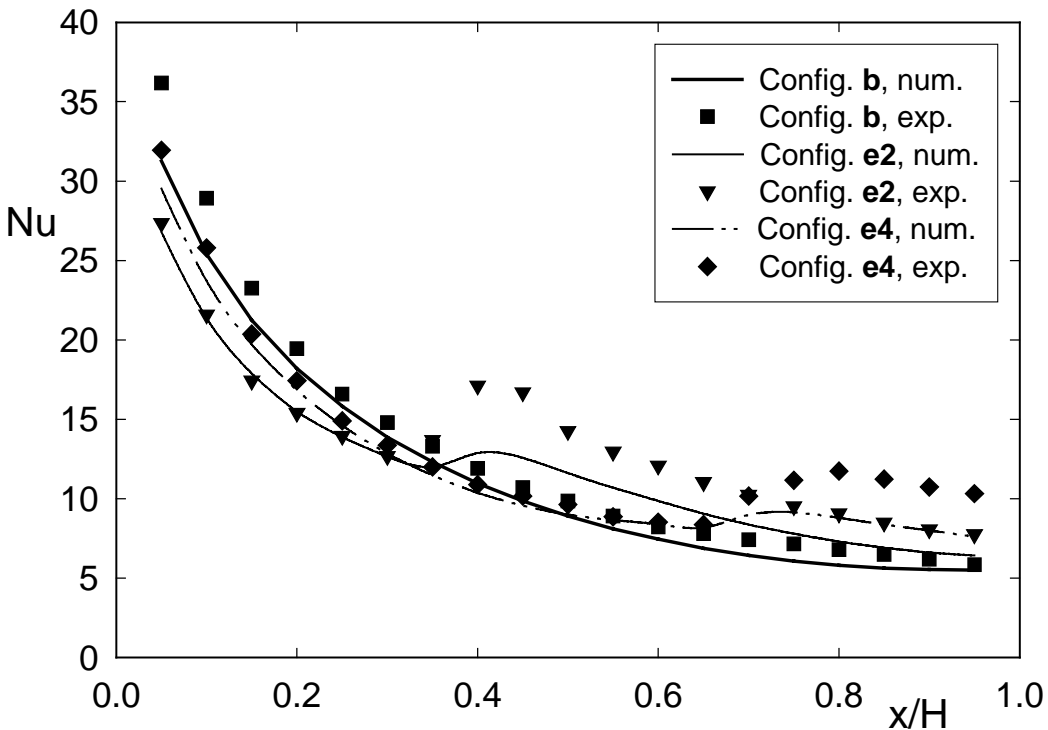


Figure 8. Comparison between local Nu number values obtained by the experiments and the numerical simulations. Config. b, e2, and e4, with thermally insulated cavity walls (I case), $Ra = 2.2 \times 10^6$.

the calculated Nu values is generally reduced when compared with the experimental results.

The flow field features are revealed by Fig.9 where numerically computed streamlines are plotted. The computed mass flow rate (per unit length L) entering the bottom opening passes from 0.35×10^{-3} kg/(s m) for the config. **b** (Fig.9a) to 0.27×10^{-3} kg/(s m) for the config. **e2** (Fig.9b) and to 0.32×10^{-3} kg/(s m) for the config. **e4** (Fig.9c). As expected, the total mass flow rate drawn into the channel is approximately the same ($0.35\text{-}0.37 \times 10^{-3}$ kg/(s m)) for all the three configurations considered. Similar results were obtained in (11) for a similar geometry and using water as the working fluid.

Figure 10 shows the average Nusselt number Nu_{av} for the largest and the smallest cavity as a function of the Rayleigh number Ra. Various symbols refer to the configurations (**a-d**) given in Table 1. Closed symbols denote lateral walls made of Plexiglas with thermal insulation (*I*), while open symbols refer to lateral walls of Plexiglas without insulation (*N-I*).

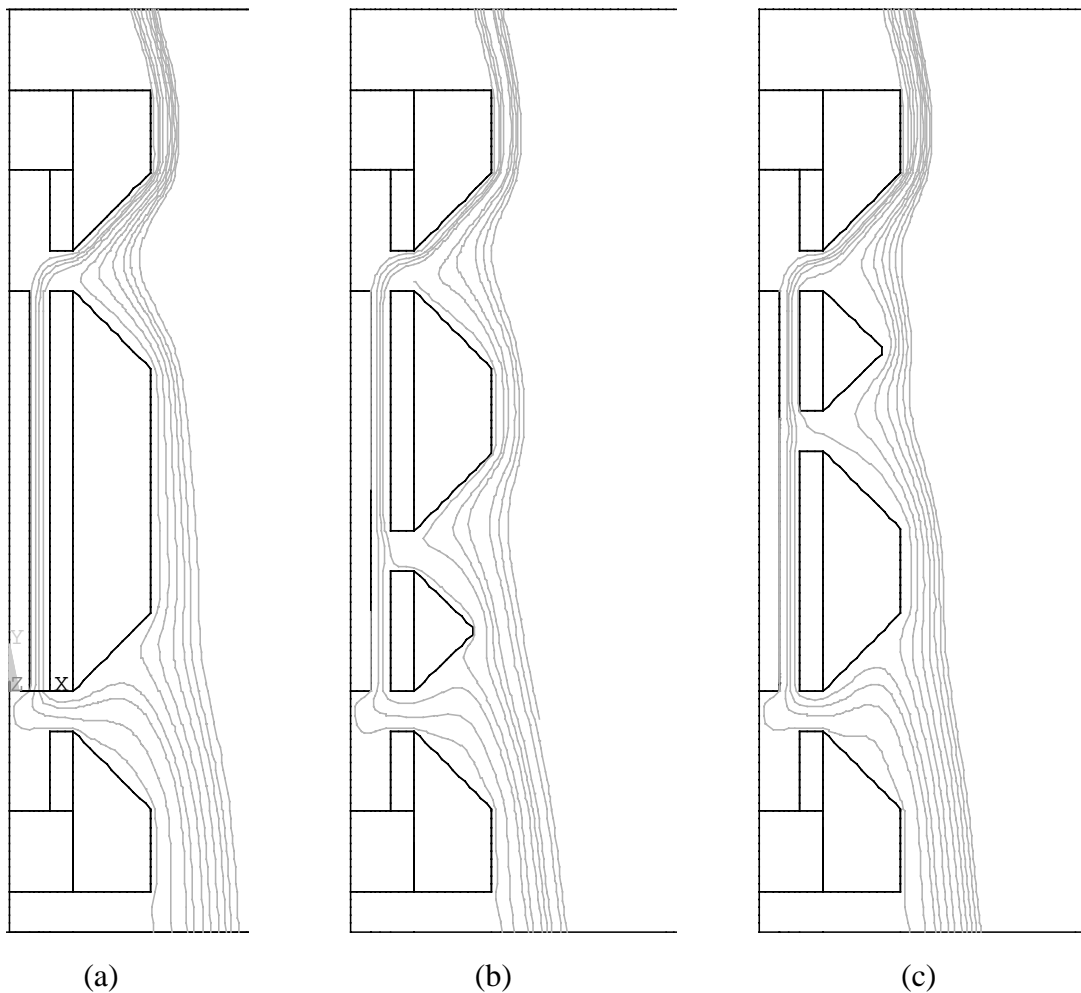


Figure 9. Computed streamline patterns for: (a) config. b, (b) config. e2, (c) config. e4. Cavity with thermally insulated walls (*I* case), $Ra = 2.2 \times 10^6$.

When the lateral walls are sufficiently far from the heated plate ($W/H=0.21$, Fig. 10a), the majority of data measured in the presence of the two rectangular openings on each side are in general slightly affected by the opening height and approach (within 10%) the results obtained for the vertical plate directly exposed to the ambient air, without the cavity walls (solid line in the figure). Only in the case

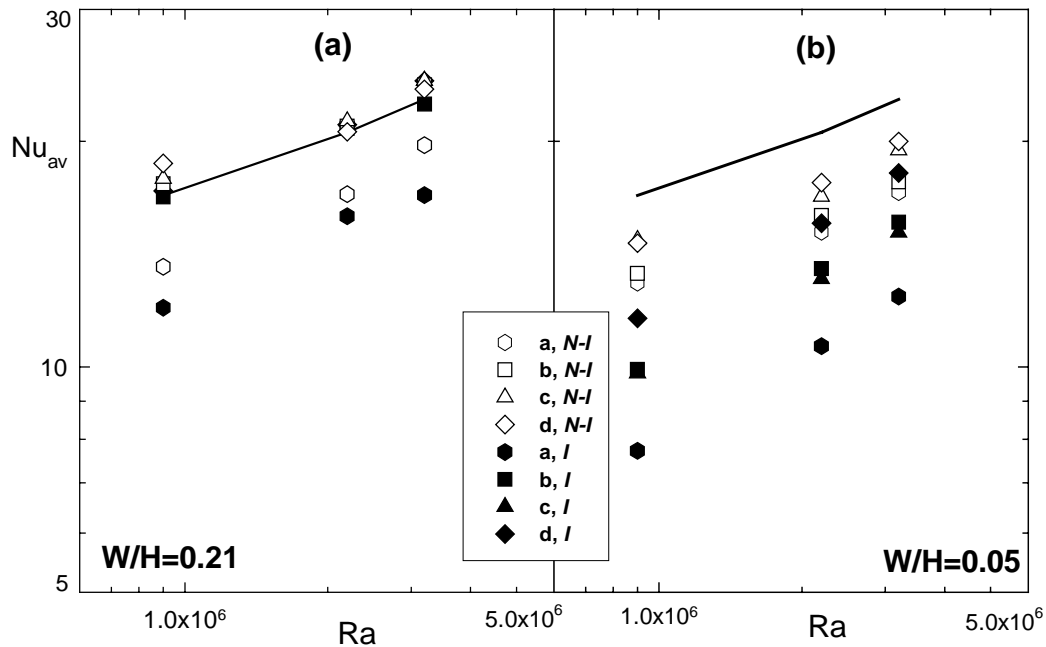


Figure 10. Average Nusselt number Nu_{av} versus Ra number: effects of the height of the openings for (a) $W/H=0.21$ and (b) $W/H=0.05$ (solid line: results for the unbounded vertical plate).

of the smallest opening height $H'=0.5$ cm (config. **a**) do results fall below the solid line. The conductance of the lateral wall does not affect heat transfer results, except again for configuration **a** ($H'=0.5$ cm), where lateral thermal insulation further reduces the overall heat transfer rate.

The results obtained for the lowest interwall spacing ($W/H=0.05$, Fig. 10b) show different features. The interaction between the thermal boundary layers growing along the heated plate surfaces and the opposite unheated walls causes marked reductions in average Nusselt numbers in comparison with the previous case. If the results for the unbounded vertical plate (solid line) are used as a reference, Nu_{av} typically decreases by 15-25% when the lateral walls are not thermally insulated (N-I case) and by 20-50% when they are (I case). In the latter case, a noticeable influence of the rectangular opening height was found: as expected, the largest height value ($H'=2$ cm, config. **d**, I case) allows a larger amount of cool air to flow inside the cavity, thus enhancing the convective heat exchange. Finally, the Nusselt number Nu_{av} averaged over the whole plate turned out to be practically

insensitive to the presence of the third opening for all the values of Ra here considered; therefore its presentation was omitted.

Figure 11 shows the channel Nusselt number Nu_{ch} as a function of the channel Rayleigh number Ra_{ch} , plotted for all the configurations (**a,b,c,d**) with (*I* case, closed symbols) and without (*N-I* case, open symbols) thermal insulation. Results are compared with the composite equation obtained by Bar-Cohen and Rohsenow (12) for an asymmetrically heated (at uniform wall temperature) vertical channel open at the bottom and top:

$$Nu_0 = (144/Ra_{ch}^2 + 2.873/Ra_{ch}^{0.5})^{0.5}$$

Inspection of the figure reveals good agreement between the majority of experimental data and the Bar-Cohen and Rohsenow equation despite the different geometry considered here. Data falling markedly below the composite equation are characterised by low values of the ratio between the opening height H' and the interwall spacing W : in this case the reduced size of the inlet/outlet opening acts as a supplementary flow resistance that penalises the heat transfer efficiency. A deeper analysis of data recorded for the thermally-insulated cavity (*I* case) has suggested the identification of

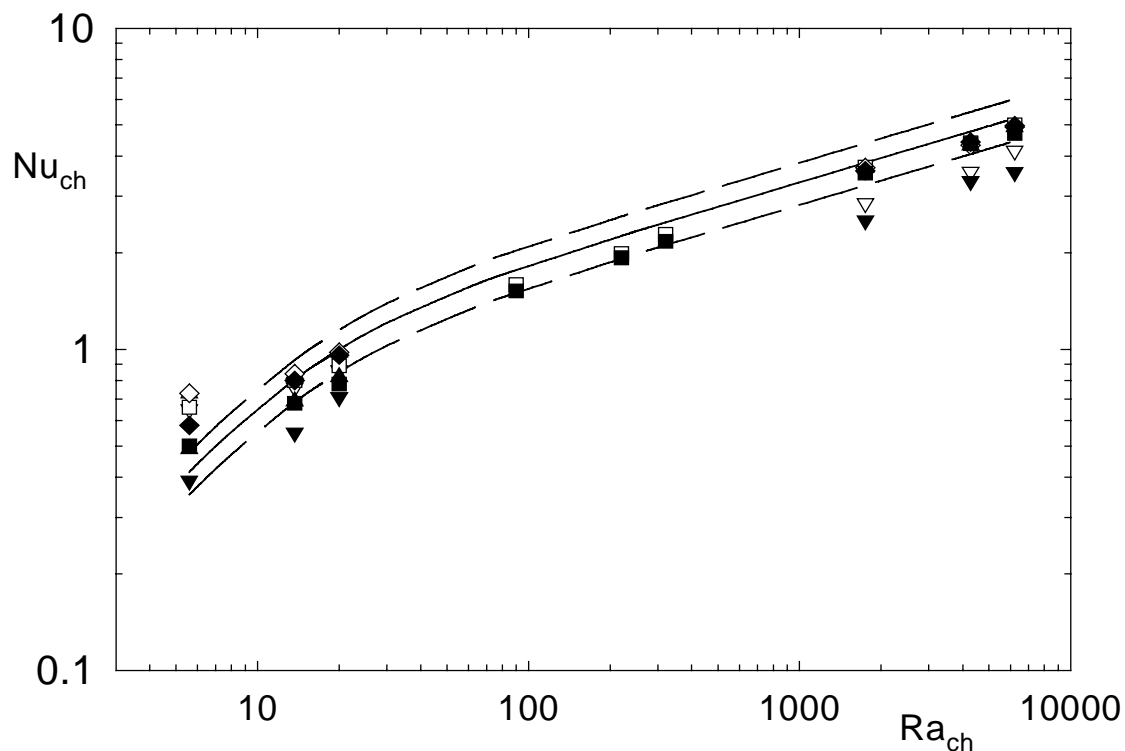


Figure 11. Channel Nusselt number Nu_{ch} against the channel Rayleigh number for the cavity configurations (a-d). Open symbols: cavity walls without thermal insulation (*N-I* case), closed symbols: cavity walls with thermal insulation (*I* case); solid line: Nu_0 (Ref. 12), the dashed lines define the $\pm 15\%$ range.

a critical value of the term $Ra_{ch}(H'/W)^3=(W/H)(\beta g/v\alpha)H'^3(T_w-T_\infty)$ beyond which the agreement between Nu_{ch} and Nu_0 is confined within $\pm 15\%$. As shown in Fig.12, where Nu_{av}/Nu_0 is reported, when $Ra_{ch}(H'/W)^3$ is approximately higher than 200, all experimental data fall within the ± 0.15 line. Therefore, the Bar-Cohen and Rohsenow equation can be used to predict the average heat transfer coefficient for the cavity (with adiabatic lateral walls) within the following parameter ranges:

$$Ra_{ch}(H'/W)^3 > 200$$

$$10 < Ra_{ch} < 10000$$

$$0.05 < H'/H < 0.2$$

$$0.05 < W/H < 0.21$$

$$0.48 < H'/W < 4.0$$

When $Ra_{ch}(H'/W)^3$ is lower than 200, the flow blockage effects induced by the vents tend to reduce the heat transfer performance of the vertical plate.

These findings could be useful in the choice of the appropriate geometric parameters (H , W , H') of the vented channel for a given wall-to-ambient temperature drop.

Conclusions

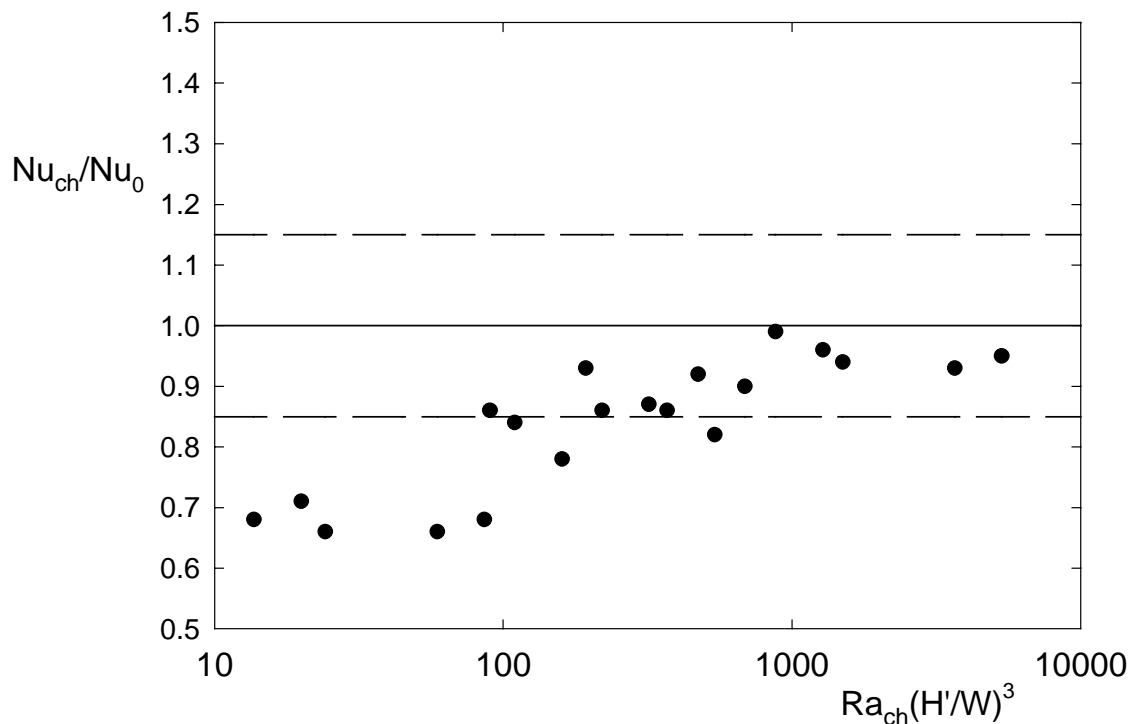


Figure 12. Channel Nusselt number Nu_{ch} (relative to the value Nu_0 given in Ref. 12) against the “modified” channel Rayleigh number $Ra_{ch}(H'/W)^3$.

Local and average heat transfer from a vertical plate inside a partially open cavity has been investigated. Nusselt numbers were determined for parametric variations of the cavity width, the plate-to-ambient temperature difference, and the number, size, and location of vent openings. The effect of the thermal conductance of the cavity side walls was also investigated. Experiments were conducted by using the schlieren optical technique to reconstruct the thermal field in the fluid and the local heat transfer coefficients at the wall. Results for the largest cavity demonstrate that heat transfer characteristics are only slightly affected by the number, location and size of the rectangular openings for the range of parameters investigated. When the cavity width is reduced, the individual height of each opening and especially the thermal conductance of the cavity walls play an important role. A third vent opening, in addition to the two main openings on each side of the cavity, causes a relative maximum in local Nu distributions in response to the relatively cool air passing through it; this circumstance was confirmed by the numerical simulations performed by a finite-element code. A composite equation, reported in the literature, giving the channel Nusselt number for an asymmetrically heated vertical channel, was found to be in good agreement with average heat transfer results obtained for the partially open cavity when the modified Rayleigh number $(W/H)(\beta g/\nu\alpha)H'^3(T_w-T_\infty)$ is approximately higher than 200.

Acknowledgements

This work was supported by Grant "Cofinanziamento MURST 97-98 - Progetto Termofluidodinamica mono e bifase".

Nomenclature

D	heated plate thickness
k	thermal conductivity of air
g	gravitational acceleration
h	heat transfer coefficient
H	heated plate height
H'	rectangular opening height
H''	additional rectangular opening height
H _c , W _c , L _c	cavity inner dimensions
L	heated plate length
Nu	Nusselt number
Ra	Rayleigh number
T	temperature
x	vertical coordinate along the heated plate
W	spacing between the heated plate and the cavity walls
α	thermal diffusivity of air

- β thermal expansion coefficient of air
 θ dimensionless temperature
 ν kinematic viscosity of air

Subscript

- _{av} average
_{ch} channel
_{in, mid, out} coordinates identifying the positions of the rectangular openings
_w plate wall
_∞ ambient air

References

- 1) Akbari, H., Borgers, T.R. "Free convective laminar flow within the Trombe wall channel" *Solar Energy*, Vol.22, pp.165-174, 1979.
- 2) Ben Yedder, R., Bilgen, E. "Natural convection and conduction in Trombe wall systems", *Int.J.Heat Mass Transfer*, Vol.34, pp.1237-1248, 1991.
- 3) Fleming, J., Ruhul Amin, M. "Conjugate natural convection in a planar thermosyphon with multiple inlets- I. Velocity and temperature fields" *Int.J.Heat Mass Transfer*, Vol.39, pp.49-59, 1996.
- 4) Fleming, J., Ruhul Amin, M. "Conjugate natural convection in a planar thermosyphon with multiple inlets- II. Heat transfer" *Int.J.Heat Mass Transfer*, Vol.39, pp. 61-68, 1996.
- 5) Gan, G. "A parametric study of Trombe walls for passive cooling of buildings" *Energy and Buildings*, Vol. 27, pp. 37-43, 1998.
- 6) Machin, A.D., Naylor, D., Harrison, S.J., and Oosthuizen, P.H. "Experimental study of free convection at an indoor glazing surface with a Venetian blind" *HVAC&R Research*, Vol. 4, pp. 153-166, 1998.
- 7) Khedari, J., Kaewruang, S., Pratinthong, N., and Hirunlabh, J. "Natural ventilation of houses by a Trombe wall under the climatic conditions in Thailand" *Int. Journal of Ambient Energy*, Vol. 20, pp. 85-94, 1999.
- 8) Misale, M. "Some considerations on practical formulas used for thermal design of natural ventilated enclosures" *Proc. Eurotherm No.29* , pp.85-94, 1993.
- 9) Tanda, G. "Natural convection heat transfer from a staggered vertical plate array" *ASME J. Heat Transfer*, Vol.115, pp.938-945, 1993.
- 10) Tanda, G., Devia, F. "Application of a schlieren technique to heat transfer measurements in free convection" *Experiments in Fluids*, Vol.24, pp.285-290, 1998.
- 11) Azevedo, L.F.A, Sparrow, E.M. "Natural convection in a vertical channel vented to the ambient through an aperture in the channel wall" *Int.J.Heat Mass Transfer*, Vol.29, pp.819-830, 1986.
- 12) Bar-Cohen, A., Rohsenow, W.M. "Thermally optimum spacing of vertical, natural convection cooled, parallel plates" *ASME J.Heat Transfer*, Vol.106, pp.116-123, 1984.